Energy conversion by autonomous regulation of chaos: Dynamical mechanism of loose coupling

Naoko Nakagawa[a)]
Department of Mathematical Sciences, Ibaraki University, Mito, Ibaraki 310-8512, Japan

Kunihiko Kaneko
Department of Pure and Applied Sciences, College of Arts and Sciences, University of Tokyo, Tokyo 153-8902, Japan

Teruhisa S. Komatsu
Department of Physics, Gakushuin University, Mejiro, Toshima-ku, Tokyo 171-8588, Japan

Inspired by recent experiments of molecular motors, a dynamical systems model for a flexible machine is proposed which converts injected energy to output directional motion. The output amount is distributed broadly, and thus the coupling between input energy and output motion is loose, as in the experiments. This energy conversion is shown to be robust against the change of surrounding environment. Stability analysis on the fixed point solutions of the model is presented, which suggests that transient chaotic motion, induced by temporal three-body motion, is relevant to the energy conversion. © *2003 American Institute of Physics.* [DOI: 10.1063/1.1594511]

How is energy converted from one form to another in order for a molecular machine to work? This question was addressed by Oosawa, who proposed that the coupling from chemical energy to mechanical work is not tightly fixed, but rather loose, in order that the molecular machine works under large thermal fluctuations although the amount of input energy is as small as an order of thermal fluctuations. Inspired by this problem, we propose a fluctuating flexible machine described by a dynamical system with a few degrees of freedom, composed of a head with internal degrees of freedom, and a lattice. By numerical simulations of this simple model, we find that after excitation of some part of the system, energy is stored for some time, and is used step by step, allowing the head to move directionally along the lattice. The system can adjust the timing for its motion by itself, by taking advantage of internal dynamics. The obtained results provide a theoretical description for dynamics of the above "loose coupling" mechanism. The head motion along the lattice by crossing over an energy barrier is achieved by changing effective degrees of freedom autonomously, as studied in chaotic itinerancy. Although we use a specific model, the proposed mechanism is expected to be rather general and is applicable to other energy conversion problems on molecular scales, including nanomachines or biological processes at such scales.

I. INTRODUCTION

Living systems often reveal rapid adaptation to fluctuating environment without any external control. Such adaptability is one characteristic feature distinguishing a living system from most man-made machines which function in a given environment under external operation by supervisors. For a system without external operations to work, adaptation to a variety of conditions should emerge through its self-organized dynamics. A dynamical systems mechanism allowing for such autonomous, flexible systems should be searched for.

In microscopic biological processes such as biochemical reaction, thermal fluctuations of the configuration of biomolecules are so large that they are of the same order of the input energy. Indeed, the input energy necessary for molecular motors to work is as small as several times of $k_B T$ with Boltzmann constant k_B and temperature T, belonging to the thermal energy regime. This is in strong contrast to a solid macroscopic machine where the input energy is much larger than the microscopic thermal fluctuations. In addition, each part of a machine also changes by itself in a biological system. For example, proteins fluctuate their own shapes slowly. Such a "flexible" machine which functions under large fluctuations is expected to have a different mechanism from macroscopic solid machines, and the mechanism should be identified. To clarify such mechanism in terms of dynamical systems, we introduce a Langevin dynamical systems model (with weak damping and noise) which allows us to explore a mechanism to function under large fluctuations of configuration.

The present paper is organized as follows. In Sec. II, we review a basic concept for such flexible machines, i.e., loose coupling between the input energy and output motion. In Sec. III, a dynamical system model is proposed for such loose coupling, inspired by some of the recent experiments on molecular motors. Numerical results demonstrating directional motion are reviewed in Sec. IV, with a broad step distribution of outputs that is consistent with the experimental data. Dynamical process achieving such directional motion is reported in Sec. V. To give a basis to resolve the

---

[a)]Electronic mail: nah@mx.ibaraki.ac.jp

behavior of the model, fixed point solutions and their bifurcations are obtained in Sec. VI, and the linear stability analysis for such solutions is given in Sec. VII. Using these results, the mechanism that enables the directional motion is proposed, by noting dynamical changes of effective degrees of freedom, and crossing over a saddle point by transient chaos. Discussion is given in Sec. VIII, with the relationship of the present dynamics with chaotic itinerancy.

II. LOOSE COUPLING

The concept of a flexible machine that works under large thermal fluctuations was proposed by Oosawa in 1986 as *loose coupling*,[1,2] to interpret experimental data of bacterial flagellar. There, it is proposed that the conversion of chemical energy to mechanical work does not occur all at once, but step by step. Conversion from chemical to mechanical energy is not tightly determined, but its rate changes event by event, and the amount of output work is distributed. The relevance of such loose coupling to flexible response of proteins under fluctuating environment is discussed.

Recent experiments of molecular motors, such as Acto-Myosin systems, demonstrate this loose coupling. There, conversion of chemical energy to mechanical one is carried out as a directional motion coupled to ATP hydrolysis for microscopic transport. Using advanced techniques in single molecule measurements, it is found that output directional motion of biomotors is a few steps per one ATP hydrolysis,[3] and that this output is distributed. The result shows clearly that the mechanical output has *loose coupling* to the input chemical reaction.

The single molecule analysis also sheds light on adaptive function of biomotors for the selection of force to carry a load. For a light load, the motor moves a few steps per one ATP hydrolysis, whereas it moves at most one step for a heavy load.[4] This indicates that the biomotor can control the force to carry the load and the amount of steps by itself. This is in contrast to the solid machine like a gear, where the input energy and the output work are both quantized and have one-to-one correspondence.

Simultaneous observation of the binding of ATP and the motion of myosin head suggests that the input energy from ATP is stored in the protein for a long interval before it is used for the directional motion.[5] The stored time scale even reaches subseconds in some cases, that is anomalously long, compared with the scale of vibrational mode in protein. Both the storage time and the step size of directional motion (corresponding to the number of functional cycles) have broad distributions. The energy storage might imply flexible adaptation of proteins, since the protein could wait for a suitable timing and fluctuation during the stored state, to realize function.

As discussed so far, a system with loose coupling will easily adapt to changes in external conditions, and will be robust to fluctuations. In this paper, we construct an explicit example of such system with self-organized dynamics, to put the abstract concept of the loose coupling into shape.

III. MODEL

To construct a flexible machine, we refer to a molecular motor system with a motor protein and a chain of rail proteins. Here we introduce a dynamical system composed of several degrees of freedom. The system has an "input part" to which energy is injected, and an "output part" from which directional motion (mechanical work) can be extracted. Temporal evolution of the system is given by a set of equations with nonlinear dynamics with damping and noise coming from a heat bath. From numerical simulations, it is shown in following sections that a directional motion is extracted, among all the degrees of the system, with neither external control nor specific control as to the timing or direction of input.

At first, we note that the present study is not directly intended to give a realistic and detailed model for molecular machine, although the study is inspired by recent experiments on protein motors, a possible relationship to which will be discussed later. Rather, in this paper, we intend to propose a dynamical description of loose coupling and autonomous energy transduction, in general. The model is adopted to give a simple illustration of the proposed mechanism.

The model system consists of a motor that interacts with a chain composed of N-lattice sites, positioned at x_i with index i. The motor consists of a "head" of position x_h and one internal degree of freedom in the form of a "pendulum" represented by θ. The injection of energy into the system is represented by the transfer of energy to this pendulum as an instantaneous increase of kinetic energy to E_0. The interaction potential $V(x_h - x_i, \theta)$ between the chain and the head is spatially asymmetric and its form depends on the angle of the pendulum (see Fig. 1). The periodic lattice is adopted as the chain, to study directional motion in an asymmetric periodic potential, as is often studied in the study of thermal ratchets. Every degree of freedom, except for the internal pendulum, is in weak contact with a heat bath, described by a Langevin equation.

The equations of motion for this system are chosen as

$$m_c \ddot{x}_i = -\gamma \dot{x}_i + \sqrt{2\gamma T}\xi_i(t) - K_c \left\{ (x_i - iL) \right.$$

$$\left. + \left(x_i - \frac{x_{i-1} + x_{i+1}}{2} \right) \right\} - \frac{\partial V(x_h - x_i, \theta)}{\partial x_i},$$

$$m_h \ddot{x}_h = -\gamma \dot{x}_h + \sqrt{2\gamma T}\xi_h(t) - \sum_i \frac{\partial V(x_h - x_i, \theta)}{\partial x_h}, \quad (1)$$

$$m_\theta \ddot{\theta} = -\sum_i \frac{\partial V(x_h - x_i, \theta)}{\partial \theta},$$

where T is the temperature, γ is a friction coefficient, and $\xi_\alpha(t)$ represents Gaussian white noise. Here, we use the units Boltzmann constant $k_B = 1$. K_c and L are the spring constant and the natural interval between two neighboring lattice sites in the chain. To observe directional motion of the head, the chain is also connected to a fixed ground via a spring with a constant K_c. Here, m_c, m_h, and m_θ are mass of the respective degrees of freedom, $m_c = m_h = 1$ and $m_h = 0.01$.
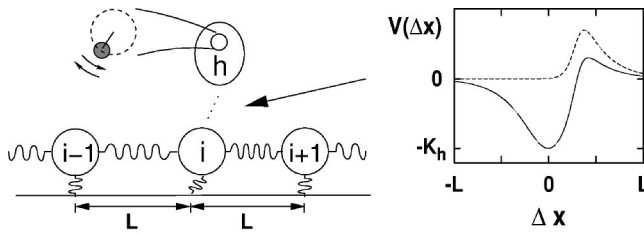
FIG. 1. Profile of the model. The form of potential V depends on the value of θ, where the solid curve represents the form for $\theta=0$ (the equilibrium state for θ), and the dotted curve for $\theta=\pi$. The latter value appears upon excitation, consisting of the instantaneous increase to E_0 of the kinetic energy for the pendulum. In the simulation of this paper, the chain consists of 40 lattice sites with periodic boundary condition.

FIG. 2. Frequency distribution of the displacement (number of steps) of the head position x_h per excitation. $K_c=0.5$, $T=0.02$, and $E_0=0.4$.

The inertia is not ignored, as small friction coefficient γ is adopted. This is in contrast to most studies where biomotors are usually treated as overdamped systems, considering that for a small object that moves with a slow time scale, water is highly viscous fluid (Reynolds number $<10^{-4}$). We introduce inertia term, since several experimental results by Yanagida's group may not necessarily match with this standard view.[3–8] First, several single-molecule experiments suggest that the fluctuations in the slow time scale as millisecond or second. For instance, Ishijima *et al.*[5] showed anomalously long-term energy storage in molecular motors. There the chemical energy from ATP hydrolysis is stored in the motor for $0.1–1$ s and then the energy is used for the directional motion gradually. If one assumes overdamped motion, such excited energy should be damped within a nanosecond or so. On the other hand, the stepping motion of protein itself (say Kinesin) could occur even in nanosecond order[7] while the waiting time before stepping is milliseconds. Compared with very slow time scales, the dynamics to realize directional motion is considerably rapid. If the water around a protein is treated just as macroscopic water, the rapid motion of the motor (for instance 10 nm by 1 ns) suggests the Reynolds number 0.1 or so, while it is not sure if the nature of water around the molecules could be just treated as such, and the effective Reynolds number could be much higher. To sum up, it is still open if the motion of molecular motor should be totally overdamped, and therefore it is interesting to consider a system with inertia theoretically.

Furthermore, each degree of freedom we used in the model does not necessarily represent an atomistic motion. Rather, it may represent a collective variable consisting of a large number of atoms. For example, a protein includes a large number of atoms. To understand energy transduction with such a large molecule, it is important to use a reduced model with a smaller number of degrees of freedom representing a collective mode consisting of a large number of atoms. It should be noted that the present scheme for the energy transduction is not necessarily restricted to a Hamiltonian system (with weak damping and noise), but it is hoped that a model with overdamped dynamics will be constructed that realizes energy transduction with loose coupling by the present scheme.

The potential form is asymmetric in space as shown in Fig. 1, where the characteristic decay length of the interaction is set at a smaller value than L, so that the interaction is confined mostly to the nearest lattice sites. Here we adopt the following potential form:
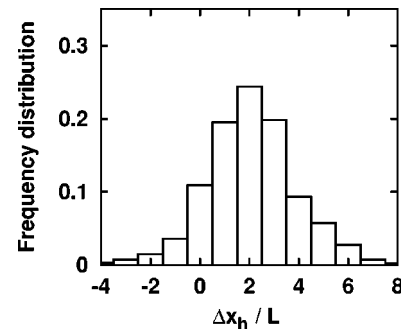
$$V(\Delta x, \theta) = K_h \frac{\tanh(p(\Delta x - r)) + (1-\cos\theta)/2}{\cosh(d\Delta x)},$$

where the parameters p and r determine the degree of asymmetry, while K_h and d^{-1} give the coupling strength and decay length of the interaction, respectively. Specific choice of this form is not important. We have simulated our model choosing several other potential forms with asymmetry, for instance $V(\Delta x, \theta) = K_h(1-\cos\theta)/(\exp(p\Delta x)+\exp(-d\Delta x))$, and obtained qualitatively the same results with regards to the directional motion. In this paper, the parameters for the potential are fixed at $p=10$, $r=0.3$, $K_h=0.2$, and $d^{-1}=0.25$.

The pendulum mode without direct coupling to the heat bath is adopted here just as one representation of long-term storage of energy[9] experimentally suggested in molecular motors.[5] This specific choice, i.e., pendulum without direct damping, is *just an example* for a long-living mode, that interacts gradually with other degrees of freedom. As long as there exists such slow relaxation mode, our results follow. Any mode realizing slow relaxation can be adopted instead.

IV. DIRECTIONAL MOTION WITH A LOOSE COUPLING TO INPUT ENERGY

In this section, we state results of the numerical integration for Eq. (1), mostly from the viewpoint of the ensemble average.

In thermal equilibrium, the head diffuses along the chain while obeying Arrhenius' law, and no directional motion is possible on average. However, when energy is imported to the pendulum and the system is out of equilibrium, directional motion is observed on its way in the relaxation to thermal equilibrium. The degree of thermal fluctuations of the system depends on flexibility K_c besides temperature T, which is larger for smaller K_c or higher T.

For a given value of E_0, we computed the distribution of the number of steps as displayed in Fig. 2, where one step means the displacement of the head for one lattice site along the chain. Here, the distribution was obtained by taking 1000 samples with arbitrarily chosen different configurations of the system at the moment of energy injection, while satisfying thermal equilibrium, and also by taking different random
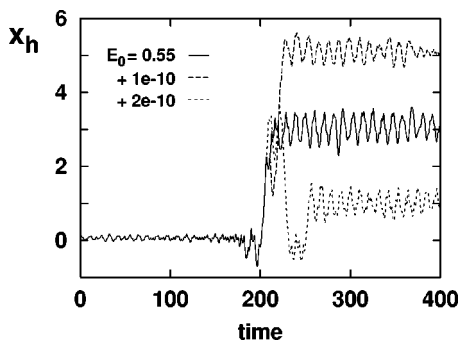
FIG. 3. Sensitivity of the dynamics to small disturbances. Three time series of the head position x_h are plotted, using the identical initial condition and common random sequence for the noise, and changing only slightly the value of excitation of the pendulum at $time = 0$, as $E_0 = 0.55$, $0.55 + 10^{10}$, $0.55 + 2 \times 10^{10}$. In the simulation, the system was prepared in thermal equilibrium before excitation with $T = 0.01$ and $\gamma = 0.01$. The tiny difference at the excitation event is amplified to large difference of the motion of the head x_h.

FIG. 4. Dependence of the average displacement $\langle \Delta x_h \rangle$ on K_c for $T = 0.01$ with three values of E_0. Directional motion is most prominent in a particular range of stiffness of the chain ($K_c \approx 0.5$), where the fluctuations of the lattice are slightly larger than those of the head. The directional motion is suppressed both for larger values of K_c, where the magnitude of lattice fluctuations decreases, and for smaller values of K_c. The latter suppression appears, because the head interacts not only with the lattice site at which it is positioned, but also with neighboring sites, resulting in a stronger effective potential experienced by the head.

sequences $\xi_\alpha(t)$. This distribution shows that the head moves directionally along the chain on average, and that the output number of steps, in which its peak value is two steps, has loose coupling to input energy. This distribution form of steps is similar to that observed in experiments of biomotors.[3]

The resulting distribution forms a rather broad shape, although the input energy E_0 is identical for all the samples. The difference in the output step comes from difference of the configuration at the event of excitation, intrinsic chaotic dynamics of the system, and random noise from the heat bath. Here we examine orbital instability (by transient chaos) as follows: Take two identical initial configurations, and put input energy whose magnitude differs slightly for each other. The temporal evolution from these samples is simulated by choosing identical random noise (i.e., sequence of random number). Then, the evolution of these systems with tiny difference in input results in quite different number of output steps (see Fig. 3). Such difference also appears from the tiny difference in initial configurations. Now, it is impossible to predict or control the number and the direction of steps from the configuration of the system at the excitation, including the direction of the rotation of the pendulum. On the other hand, the directional motion appears rather independently of the configuration and, therefore, the energy conversion of the system is robust against thermal fluctuations in configuration, and fluctuations in the input event.

The output directional motion is also robust against changes in the environmental temperature, while higher temperature brings larger fluctuations to the system. Furthermore, the average number of steps increases monotonically with the amount of injected energy.[10] In other words, the more input energy, the more it is used for the output motion. The system can adjust itself to the change of input energy through its internal dynamics, even under large fluctuations in configuration. To make this energy conversion possible, it is important that the chain be sufficiently flexible and be fluctuated in large range thermally or excitedly. If the spring constant K_c is too large or too small, directional motion of the head is scarcely generated (see Fig. 4). This feature is

commonly observed against the change of other parameters. The condition for the flexibility in the spring will be revisited later from the viewpoint of stability analysis.

V. DIRECTIONAL MOTION WITH THE USE OF EXTRA DEGREES OF FREEDOM

Now, we discuss how energy conversion to the directional motion is carried out, by closely examining the dynamics of the model. Figure 5 displays a typical time sequence of the head x_h, a few lattice sites x_i around it, and the kinetic energy T_θ of the pendulum after an event of excitation at $time = 0$. We here introduce characteristic behavior of the system depicted as (a)–(d) at the time sequence in Fig. 5. The configuration of the system at each stage is schematically represented in Fig. 6.
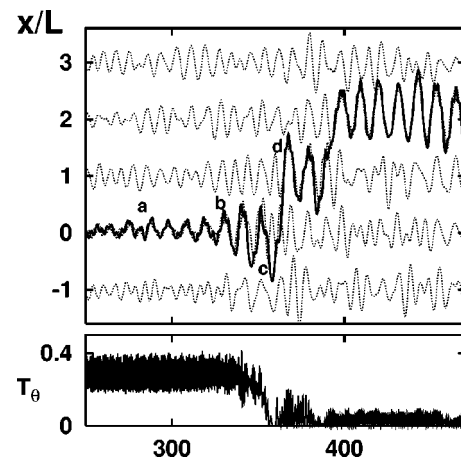
FIG. 5. A typical relaxation process following excitation of the pendulum. $K_c = 0.5$. In the simulation, the system was prepared in thermal equilibrium with $T = 0.02$ and $\gamma = 0.01$, and the pendulum was excited at $time = 0$ with $E_0 = 0.4$. With the temperature used here, the head remains at one lattice site for a very long time in thermal equilibrium. Upper panel: Time series of the positions of the head x_h (bold line) and a few neighboring lattice sites x_i ($-1 \leq i \leq 3$; dotted line). Lower panel: Time series of the kinetic energy of the internal pendulum (T_θ). In the upper panel, the index (a)–(d) corresponds to each stage schematically shown in Fig. 6.
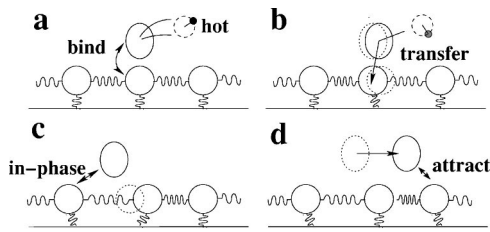
FIG. 6. Schematic representation on the directional motion. The reference index (a)–(d) corresponds to each stage shown in the time sequence in Fig. 5.

When the pendulum motion is fast, and is essentially decoupled from the head motion, the head and the nearest lattice site bind strongly and they exhibit highly correlated vibration [at stage (a)]. This correlation is especially remarkable in a weak spring case where K_c is small compared to the coupling by the potential V. There, the motion of the head and the nearest site is governed mainly by a two-body interaction between x_h and x_0, via the attractive potential $V(x_h - x_0)$, which induces this coherent vibration. The complex consisting of the head and the lattice site 0 behaves as if they are a single particle that is heavier than other sites (i.e., moves with a slower time scale motion). Indeed, this "particle," consisting of the lattice site and the head, is coupled to the neighboring sites, and they show roughly periodic oscillation. Here, the motion of the head and lattice sites are just combinations of two-body vibrational motions.

Since the pendulum interacts with the other degrees of freedom, it does not rotate completely freely, even though the rotation is fast. As the rotation is slowed, the pendulum motion starts to influence the head motion, due to the nonlinearity of the potential $V(x_h - x_i)$. The pendulum motion is no longer decoupled from the rest of the system, and the pendulum, the head, and the corresponding lattice site come to exhibit three-body motion. As shown in Fig. 3, the motion of the system starts to show highly chaotic motion, which induces irreversible relaxation.[11] At this stage, the energy from the pendulum is not immediately diffused to other lattice sites, and is localized at the head and the binding lattice site for a certain interval. As a result, the vibration amplitude of the complex of the head and the site becomes larger with the energy transfer from the pendulum [stage (b)].

With the increase of the vibration amplitude, the coherent motion of the head and the corresponding lattice site is lost and they start to vibrate in antiphase [stage (c)], as the interaction with other degrees of freedom (i.e., the pendulum and neighboring lattice sites) are no longer negligible. The growth of the antiphase mode between x_h and x_0 is shown in Fig. 7(a), where the large amplitude appears for a few periods before the head moves to the next site. With the loss of coherence between x_h and x_0, the head interacts more strongly with the neighboring lattice sites to the original. The interaction that the head experiences here is highly asymmetric, i.e., repulsive with the left lattice site (x_{-1}) and attractive with the right (x_1), as given in the potential $V(x_h - x_i)$ in Fig. 1 (for the interaction with the left site see $x_h - x_i \sim L$ and for the right see $x_h - x_i \sim -L$). At this stage, the head motion becomes occasionally synchronized with that of
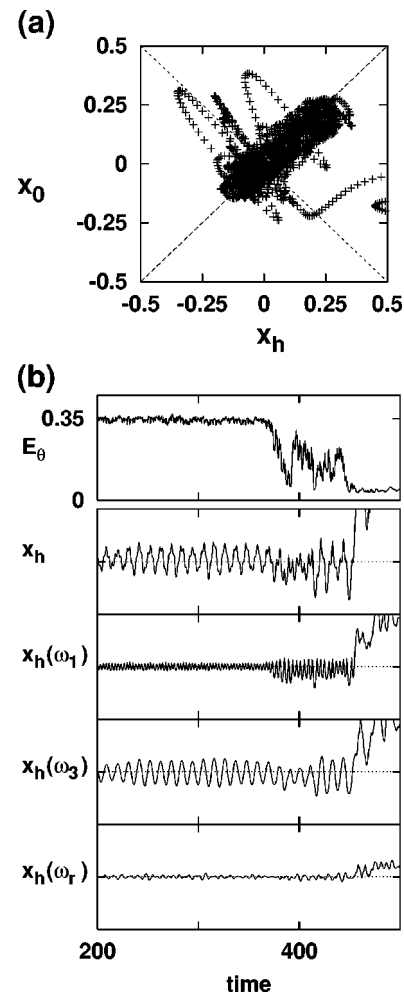
FIG. 7. (a) Plot of an orbit projected in the two-dimensional space (x_h, x_0), from an event of excitation to the step motion. At first, the head and the lattice vibrate almost synchronously, as shown by the distributed points along the line $x_0 = x_h$. In contrast to a relatively large motion of their center of mass along the diagonal line, vibration of the two-body motion $(h-O)$ is kept small, as shown in the vibration along the antidiagonal direction. As the pendulum loses energy, the amplitude of the relative motion between x_0 and x_h grows, as is demonstrated by a few periods of large amplitude vibration parallel to the line $x_h + x_0 = 0$. This corresponds to stage (c) in Fig. 5. After this swing motion of the head, the head moves to the next lattice site. (b) Eigenmode expansion of the time series of the head around the two-body solution $(h-O)$. $N = 7$, $K_c = 0.5$, $E_0 = 0.35$, $T = 0.005$, and $\gamma = 0.05$. The first column gives the relaxation of excited energy E_θ of the pendulum. The second one shows original time sequence of x_h. The third and fourth columns give the component of the ω_1 and ω_3 mode for the time series x_h, respectively, while the bottom column gives the sum of the components of other modes. The vertical axes are in the range $-1 < x_h, x_h(\omega) < 1$.

the next site to the left. Because the interaction between the head and the left lattice site is repulsive, the head bounces back eventually to the next site to the right, after a few periods of vibration [stage (d)]. Attractive interaction with the right site also enhances this bouncing-back. Through this process, the head absorbs energy from the chain, so that it can cross over the energy barrier to the next site to the right. The timing of this crossing is spontaneously determined by the interaction among the head, pendulum, and lattice sites.

For the present mechanism to function, energy must be localized within the head and neighboring lattice sites for a while.[10,12] This condition is not satisfied, for example, when
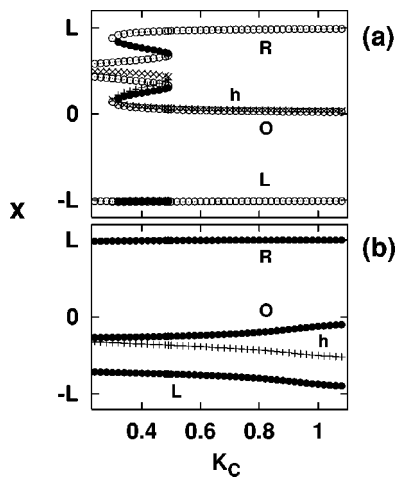
FIG. 8. Fixed point configuration of the head and the neighboring lattice sites, plotted as a function of the parameter K_c. Each fixed point solution is derived from the model equations (1) for each value of K_c. Here ($\bigcirc$) or ($\bullet$) shows the positions of lattice points (R,O,L) and ($\times$) or ($+$) that of the head. Here ($\bigcirc$) and ($\times$) display those of stable fixed points, and ($\bullet$) and ($+$) those of unstable fixed points. In branch (a), there are two bifurcation points around $K_c \simeq 0.3$ and $K_c \simeq 0.5$.

the spring is stiff (i.e., when K_c is large). In that case, energy rapidly diffuses from the binding site to other sites, and the present energy conversion does not work. As a result, the directional motion is suppressed for large values of K_c, as shown in Fig. 4. To sum up, the localization of energy at a few lattice sites near the head over some time allows for effective energy conversion, which results in directional motion. It is interesting to note that in real molecular motor, the directional motion is suppressed when the stiffness of actin filament is increased by attaching proteins to it.[13]

VI. FIXED POINT ANALYSIS

In this section, we analyze stationary states (i.e., fixed points) of Eq. (1) as a step to understand the dynamics discussed in Sec. V. For the sake of the analysis, here the excitation of the pendulum and coupling to the heat bath are removed from the model. The number of the lattice sites is reduced to be $N = 3$ with adopting a periodic boundary condition. This number is a minimum for the head to exhibit directional motion, while maintaining a common feature with that of larger systems. Then, the system to analyze has five degrees of freedom, i.e., head, three lattice sites, and the pendulum. Here we study bifurcation of the fixed points against the change of the stiffness K_c of the chain, while fixing other parameters at the values used in Sec. III. It is also noted that equivalent stationary states exist even for larger systems with $N > 3$, as a periodic repetition of the solution at $N = 3$.

First, as derived from Eq. (1), the pendulum is stable for $\theta = 0$ and unstable for $\theta = \pi$, independently of the configuration of the other degrees of freedom. Hence, among the five degrees of freedom, the fixed point condition for θ is separated out only to these two cases. We hereafter argue stationary states at $\theta = 0$ (stable case).

In Fig. 8, the three lattice points (R,O,L) and the head position (h) of the fixed point solutions are plotted with the

change of K_c. There are two branches of the solutions. Each branch is shown in Figs. 8(a) and 8(b), respectively. Here, the upper case (a) undergoes bifurcation, while the other does not [Fig. 8(b)]. Compare the head position with the lattice points in (a). Since $x_h \sim x_O$, the configuration Fig. 8(a) corresponds to a binding state with the head and the site O, while the configuration changes with the value of K_c. We call this two-body binding-state solution, or two-body solution in short. It is remarkable that this binding-state solution between the head h and the site O is stable within a wide range of K_c, as shown in the lower branch satisfying $x_h \sim x_O$ in Fig. 8(a). The branch disappears around $K_c \sim 0.3$, and it does not exist below the value. On the other hand, in the range $K_c \lesssim 0.49$, there is another (upper) sub-branch in Fig. 8(a), where h is between R and L, which are located at closer distances. We call this a three-body binding-state solution $(O-h-R)$, since the head and the sites O and R form a stable binding state.

For large K_c, the two-body solution $(h-O)$ gives a ground state, energetically speaking, that stays at a minimum in potential energy, while it is replaced by the three-body solution $(O-h-R)$ for smaller values of K_c. In the configuration of the three-body state, elastic energy of the springs gets much larger than that of the two-body binding state $(h-O)$, since the site O is very close to the site R and far from the site L. However, if the spring constant is sufficiently small, the repulsive force from the springs is compensated, by the attractive interaction between the head and the site R via $V(x_h - x_R)$, and it is negligible.

In branch (a), there is another unstable fixed-point solution around $0.3 < K_c < 0.5$, which coexists with two stable solutions. It is a saddle point dividing the two stable solutions.

The stationary solution of the branch (b) is unstable over the whole range of K_c displayed in Fig. 8(b). It is a saddle point to divide two translationally invariant solutions, that exists due to the spatially periodic structure of the model equations. This is easily understood by considering the situation with a large K_c limit, where lattice sites are almost fixed to the periodic point $x_i = iL$. Then dynamical behavior of the system is determined solely by the motion of the head, which is located in a periodic potential. The head is stable at the point of global minimum for the potential around $x_h = iL$, and unstable at a saddle point within $i < x_h < i + 1$. The difference between the potential energies at the saddle point and at the ground state gives us a measure of the energy barrier for the head to shift to the next lattice site. This corresponds to activation energy for the head to move along the chain. Indeed, the energy barrier estimated here, for each value of K_c, is consistent with the values defined from the Arrhenius law for the diffusion of the head, which is obtained by the numerical simulation at thermal equilibrium condition.

The bifurcation point for the emergence of the three-body solution $(O-h-R)$ is important. As is seen in Fig. 4, the average step of the head takes the largest value around this bifurcation point in K_c. It is suggested that the dynamics to generate the three-body motion $(O-h-R)$ is correlated with the directional motion to go across the energy barrier.
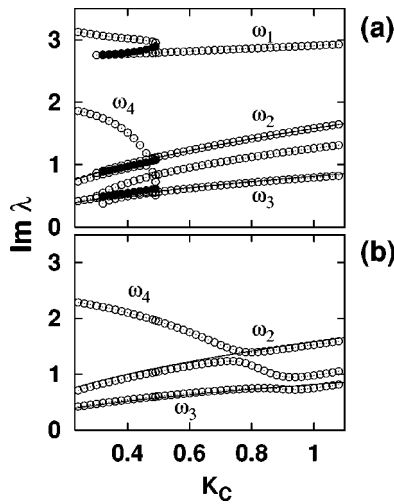
FIG. 9. Eigenfrequencies for each eigenmode around each fixed point. In (a) four eigenvalues for the solutions in the branch (a) of Fig. 8 are displayed, while in (b) those for the branch (b) are shown. ($\bigcirc$) and ($\bullet$) show the frequencies around stable (elliptic) fixed points and unstable (saddle) points, respectively. Over the range of K_c, the relationships $\omega_2 \sim \sqrt{2K_c/3}$ and $\omega_3 \sim \sqrt{K_c/4}$ are approximately maintained, which correspond to the mode of lattice vibrations. The resonance point at the crossing of the frequency curves appears around $K_c \simeq 0.5$ (a bifurcation point) for the solution in branch (a), and around $K_c \simeq 0.75$ in branch (b).

Relaxation near the bifurcation point generally gets slower. Hence the motion of the head and lattice points gets slower near the bifurcation point of K_c. During this slow relaxation, characteristic energy flow between various modes is induced in the system, which lead to an effective energy transfer from the pendulum to the head and the lattice points, sufficient to go across the energy barrier.

VII. LINEAR STABILITY ANALYSIS

As a next step to understand the dynamics of the present system, linear stability analysis around the stationary solutions is carried out. We study frequencies of linearized motion around each fixed point, to see how switching from the motion around one fixed point to another is possible.

Since we analyze a system with five degrees of freedom, the linearized solution around each fixed point solution has five pairs of eigenvalues. Indeed, the two stable states in branch (a) are elliptic points with five pairs of imaginary eigenvalues. On the other hand, the unstable solutions in branches (a) and (b) are a saddle with one pair of real eigenvalues and four pairs of imaginary eigenvalues. Each imaginary eigenvalue gives a frequency of a corresponding vibrational mode. Here, as mentioned in Sec. VI, the stationary state of the pendulum mode is determined independently of the configuration of the other degrees of freedom. Hence we focus on the remaining four (for the stable solution) or three (for a saddle) frequencies except the pendulum mode. These frequencies are plotted in Fig. 9.

Figure 9(a) displays four (or three) angular frequencies for each solution in branch (a). Three frequencies depicted as ω_1, ω_2, and ω_3 possess common properties for all the solutions. The fastest frequency ω_1 is kept far from others and $\omega_1 \simeq 3$ over the whole range of K_c. By examining its eigen-
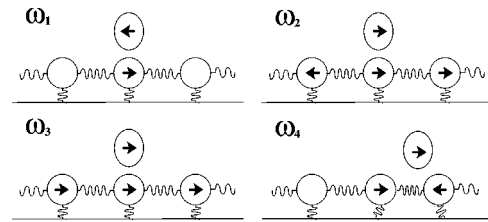
FIG. 10. Schematic representations of each eigenmode corresponding to the eigenfrequencies ω_1, ω_2, ω_3, and ω_4. The direction of each arrow indicates relative direction of the components of each eigenvector.

vector, this mode is found to correspond to the vibration between the two body, the head and the nearest lattice site O. Schematic representations for each eigenvector are shown in Fig. 10, where one can see the phase relationship between each motion (i.e., in-phase or antiphase relation) from the relative directions of arrows. In contrast, the frequencies ω_2 and ω_3 are modes of lattice vibration, which increase proportionally to $\sqrt{K_c}$. The slowest mode ω_3 corresponds to the collective, translational mode of all degrees of freedom in phase. (Since each lattice is attached to a fixed, periodic potential, the Goldstone mode does not exist, and the eigenvalue is not zero. Still, it is small.) These two lattice modes are maintained for all solutions, even in the saddle solution in branch (b) as shown in Fig. 9(b). Again, by examining their eigenvectors, it is shown that there are two eigenvectors for the solution (b), corresponding to those for ω_2 and ω_3 in (a).

In the vicinity of each stationary state, the dynamics are represented by superposition of these eigenmodes. For instance, the lattice vibration observed in stage (a) in Fig. 5 mainly comes from ω_3, which is the longest collective mode with the largest amplitude of vibration, while the fast, small-amplitude vibration between the head and the lattice O at the stage (a) comes from the eigenmode for ω_1, whose amplitude increases with the inflow of energy from the pendulum as seen at stage (c) in Fig. 5 and Fig. 7(a).

To see how each mode contributes to the directional motion of the head, we expand it into the eigenmodes, by projecting the head motion into each mode. Temporal change of the component of each mode is plotted in Fig. 7(b). Before the inflow of the energy from the pendulum, the mode of ω_3 shows a large-amplitude vibration. This is natural, since the mode of ω_3 corresponds to a two-body binding state ($h-O$). As the pendulum loses energy, the amplitude for ω_1 increases, and it becomes of a comparable order with that of ω_3. This shows the appearance of antiphase vibration. Up to this stage [i.e., up to time ~ 400 in the example of Fig. 7(b)], the components of other modes remain small, and do not affect much the behavior of the head.

Then, instability in the two-body solution ($h-O$) brings about breakdown of the binding state between the head and the site O. At stages (c) and (d) in Fig. 5, the system is excited from the ground state, and approaches the saddle in the branch (b). As seen in Fig. 10, all vibrational modes on the saddle point are in-phase motion between the head and the site O. Such vibration modes support the synchronization observed in the repulsive interaction at stage (c). Here com-

ponents from other modes are slightly increased, as shown in Fig. 7(b), right before the step motion of the head.

As the head is occasionally deviated to the right neighboring site R, the configuration becomes similar to that of the three-body binding state $(O-h-R)$ in branch (a), which exists at the range of K_c allowing for the effective directional motion. Then, to escape from such temporal three-body binding state, and to make a shift of the head to the next site, antiphase relationship between the head and the site R is important. Here, such motion is given by the eigenmode for ω_4, where the site R moves to the opposite direction to both the head and the site O (see Fig. 10). At the saddle solution in branch (a), the eigenmode corresponding to ω_4 in Fig. 9 takes a real eigenvalue, whose eigenmode gives the unstable direction of the saddle. Along the stable direction of the saddle, the head and the sites R and O are first combined, and later, along the unstable direction, the site R is departed from the binding state of the head and the site O. In other words, the system is attracted to the three-body binding state $(O-h-R)$, and then it is repelled from the state. This corresponds to stage (d) in Fig. 5. In the time series in Fig. 5, the head is shifted to the next site successively, following this attraction. The temporal attraction to the three-body state and exit from it through the saddle is important to understand how the head goes across the energy barrier to make a directional motion.

Here it is difficult to find out the growth of the mode ω_4 at the stage (c) or (d), by measurement of the components as in Fig. 7(b). We could detect the increase of the modes other than ω_1 and ω_3, as a total, but direct observation of the increase of ω_4 mode is not easy, even if we adopt the mode expansion around the three-body solution $(O-h-R)$. There can be two possible reasons here. First, the head crosses the energy barrier through the saddle within a short time scale, and the mode is too difficult to be detected. Second, around the saddle of a three-body motion, chaotic (transient) motion is generally expected, following the resonance overlapping.[14] Indeed, to fully understand the dynamics, the linear analysis is not sufficient, of course. To close the section, we briefly discuss the resonance overlapping.

Note that frequencies ω_2 and ω_4 are close around the bifurcation point of K_c in branch (a). Also, for the saddle point in branch (b), ω_4 shows a remarkable decrease with the increase of K_c, and crosses with ω_2 at a certain value of K_c, as shown in Fig. 9. When these two frequencies get close, there appears resonance between the modes, due to nonlinear terms in the original equation. In general, in a three (or more) body motion with the resonance overlap, stochastic layer is formed around the saddle point that separates two different binding states. Along the stochastic layer, chaotic motion is generated. This stochastic layer is expected to be thickened as ω_4 and ω_2 get closer, as has been generally studied.[14] Hence, with the resonance overlap, the motion to go across the saddle would be facilitated.

In our problem, it is rather difficult to demonstrate directly that chaotic motion is due to resonance overlapping, since the motion appears only as a transient motion within a short time scale. However, orbital instability as well as irregular motion is observed around the stage (c) and (d), i.e.,

between the beginning of inflow from the pendulum and the shift of the head.[12] This instability is not solely due to the inflow of energy, since the index for the instability, given by (finite-time) Lyapunov exponent, is kept constant even after the first inflow of energy finishes. Recalling generality of the resonance overlap mechanism for chaos,[14] it is rather natural to assume the existence of resonance overlapping here.

The above-presented linear analysis is argued for a special case $\theta=0$. After an excitation, the pendulum rotates and the value of θ is distributed. It should be noted that both the bifurcation point of K_c and the resonant points of K_c for ω_2 with ω_4 are shifted to smaller values of K_c, for $\theta>0$. To sum up, around $0.3<K_c<0.75$, the stochastic layer to go across the saddle would be broader and the crossing of the energy barrier would be easier. The chaotic dynamics around the saddle would destroy the correlation between the head and lattice sites, and would be relevant to induce directional motion. In relationship, it should be noted that the average shift of the head tends to have a peak around this region of K_c (see Fig. 4).

VIII. SUMMARY AND DISCUSSION

In the present paper, we have analyzed a dynamical systems model for energy transduction, inspired by recent experiments on molecular motors. Using Langevin dynamics (with inertia), it is shown that the injected energy to one of the degrees of freedom is successively converted to directional motion, under the thermal fluctuations of configuration. Before the injection of energy, the system is in equilibrium, where the stationary state is approximately decoupled into two-body motions (given by the binding state between the head and the lattice). As the stored energy into one of the degrees of freedom is dissipated, several degrees of freedom start to interact. Then, the original stationary state is destabilized, and is replaced by chaotic transient. Now the binding state between the head and the lattice is destabilized. As schematically shown in Fig. 6, the head starts to interact with the neighboring site strongly. Then, through asymmetry in the potential, directional output motion results.

One consequence of this chaotic (transient) dynamics is loose coupling between injected energy and output motion, as demonstrated by the broad step distribution. Indeed this distribution reproduces the observation in the experiment of molecular motors rather well. In general, loose coupling between the input and output motion, demonstrated by the broad distribution of output motion, is an inevitable consequence of the chaotic dynamics during the course of crossing over the potential barrier.

The present result also implies robustness of the energy transduction process. Recall that our mechanism does not rely on any specific resonance. Rather, at the crossing of the potential barrier, three (and later more) degrees of freedom are involved. Note that in Hamiltonian systems with a few degrees of freedom, the stochastic layer is formed as a result of resonance overlap. Chaotic motion arises along the stochastic layer, and an orbit crosses the saddle point with this motion, while this chaotic motion brings about a broad band of frequencies. In the present example also, stochastic mo-

tion appears to cross over the saddle point. Accordingly, the crossing behavior is robust against the change of other parameters such as the injected energy, in contrast to simple resonance, where the parameter and injected energy have to be tuned finely to satisfy the resonance condition.

As a theoretical model for molecular motors, thermal (or other) ratchets have been extensively studied.[15–17] In the ratchet model, input of energy is represented in the form of either temperature difference, switching of potential, or specific colored noise. These are external processes that the system of concern cannot change autonomously. In the present model, the temporal evolution is given only by autonomous dynamics, once the energy is injected. The input energy does not need to take a specific value, and is injected at any timing in the evolution of the system. Depending on the amount of input energy, the timing for the stabilization of the two-body binding state changes, as a result of autonomous dynamics of internal degrees of freedom. As a result, the timing for crossing the energy barrier is also adjusted so that the directional motion results on average. Indeed, the average of output step motion increases with the input energy, implying that the injected energy is not wasted out.

To close the paper, we discuss the relationship of the present dynamics with chaotic itinerancy. In chaotic itinerancy (CI), residence at low-dimensional ordered states and switching to a new ordered state through higher dimensional chaos are repeated. Here, change of effective degrees of freedom is essential to this itinerancy. Switching process from one ordered state to another is neither tightly determined nor random. Indeed, these characteristics are nothing but the features that make the robust energy conversion possible in our model.

In the present example, switching from one binding state between the head and a lattice site to another binding state appears through the change of effective degrees of freedom. Each binding state is a low-dimensional ordered state, which is destabilized under the influence of other degrees of freedom. In the present model without the coupling to the pendulum mode, the head and the lattice maintain the binding state. Only when the pendulum mode starts to interact effectively, the coherent motion between the head and the lattice is destabilized. Hence with the increase of effective degrees of freedom, the coherent motion is replaced by chaotic motion. Then, the head starts to interact with the neighboring lattice sites, leading to the further increase of the effective degrees of freedom. The head shows strongly chaotic motion then. With this ''high-dimensional'' transient motion, the head moves to a next site (or to a farther site), and eventually it forms a binding state with the lattice sites, and the coherent motion is recovered. In other words, transition from one ordered state to another occurs through the change of effective degrees of freedom for the head motion. This autonomous change of effective degrees of freedom here is nothing but that discussed in the study of CI.

When the head moves along the lattice directionally, it crosses over the energy barrier, passing through the region around a saddle point. There, three- or four-body motion is involved, and the orbit shows chaotic motion presumably along a stochastic layer formed by the resonance overlap. Then, the orbit crosses the barrier, taking advantage of the motion along the stochastic layer. Thus, the crossing from one binding state to another is neither random nor tightly determined. Recall that such transition between states through chaotic motion is an important factor of chaotic itinerancy.

In the mechanism by ratchet models, random noise gives a trigger to the transition between states. The orbit shows Brownian motion in the phase space. On the other hand, in the present mechanism, the orbit is restricted in stochastic layer around a saddle point, which facilitates the directional motion. Detailed analysis on how the transition by the present mechanism differs from the standard thermal activation process is left for future studies.

One may note that there is one difference between the present dynamics and CI. In contrast to CI, transition among ordered states is not repeated indefinitely in the present case. Still, other features are common, and in this sense, use of ''transient'' CI for energy conversion should be seriously pursued in the future. Indeed, the application of the present mechanism is not necessarily restricted to the problem of biomotor, but the mechanism can be applied in general to a system with the energy conversion using internal dynamics, such as to the function of enzymes, protein folding, and chemical reaction process.[18]

ACKNOWLEDGMENTS

[1] F. Oosawa and S. Hayashi, Adv. Biophys. **22**, 151–183 (1986).

[2] F. Oosawa, Genes Cells **5**, 9–16 (2000).

[3] K. Kitamura, M. Tokunaga, A. Hikikoshi-Iwane, and T. Yanagida, Nature (London) **397**, 129–134 (1999).

[4] A. Ishijima, H. Kojima, H. Higuchi, Y. Harada, T. Funatsu, and T. Yanagida, Biophys. J. **70**, 383–400 (1996).

[5] A. Ishijima, H. Kojima, T. Funatsu, M. Tokunaga, H. Higuchi, and T. Yanagida, Cell **92**, 161 (1998).

[6] C. Shingyoji, H. Higuchi, M. Yoshimura, E. Katayama, and T. Yanagida, Nature (London) **393**, 711–714 (1998).

[7] M. Nishiyama, E. Muto, Y. Inoue, T. Yanagida, and H. Higuchi, Nat. Cell Biol. **3**, 425–428 (2001).

[8] T. Wazawa, Y. Ishii, T. Funatsu, and T. Yanagida, Biophys. J. **78**, 1561–1569 (2000).

[9] N. Nakagawa and K. Kaneko, J. Phys. Soc. Jpn. **69**, 1255–1258 (2000).

[10] N. Nakagawa and K. Kaneko, Phys. Rev. E **67**, 040901 (2003).

[11] N. Nakagawa and K. Kaneko, Phys. Rev. E **64**, 055205 (2001).

[12] N. Nakagawa and K. Kaneko (unpublished).

[13] T. Yanagida, M. Nakase, K. Nishiyama, and F. Oosawa, Nature (London) **307**, 58–60 (1984).

[14] B. Chirikov, Phys. Rep. **52**, 263–379 (1979).

[15] R. D. Vale and F. Oosawa, Adv. Biophys. **26**, 97–134 (1990).

[16] M. O. Magnasco, Phys. Rev. Lett. **71**, 1477–1481 (1993).

[17] F. Jülicher, A. Ajdari, and J. Prost, Rev. Mod. Phys. **69**, 1269–1281 (1997).

[18] T. Komatsuzaki and R. S. Berry, Adv. Chem. Phys. **123**, 79–152 (2002); M. Toda, *ibid.* **123**, 153–198 (2002), and references therein.